Supporting information for

Multi-step PDMS Curing and Controlled Separation method for Mass Manufacturing of High-performance and User-Friendly Micro-device: Valved Micropumps

Zhichang Du,[1, 2] Wei Sun*[3] and Shengli Mi*[2]

[1] College of Mechanical and Energy Engineering, Jimei University, Xiamen, China

[2] Bio-manufacturing Engineering Laboratory, Tsinghua Shenzhen International Graduate School, Tsinghua University, Shenzhen, 518055, China

[3] Precision Medicine and Healthcare Research Center, Tsinghua-Berkeley Shenzhen Institute, Shenzhen, China

*Corresponding authors. E-mail: mi.shengli@sz.tsinghua.edu.cn

Tab. S1 Size and performance comparison of the micropump with existing valved micropumps

Types of valved micropumps	Pump membrane diameter (mm)	Estimated assembly size (mm)	Method for measuring flow rate	Measured flow rate	References
Micropump with active valves	4.1	15 × 8 × 4	A scale tracing gas-liquid interface	About 50 μL per 60 times press	1
Micropump with one-way valves	7	20 × 10 × 4	Estimating method based on driven volume	Up to 55 μL/min	2
Micropump with planar one-way valves	4.4	10 × 10 × 4	A scale tracing gas-liquid interface	180 μL/min at 30 kPa, about 35 μL/min at 9 kPa	3
The micropump with one-way valves	2.8	5 × 5 × 0.7	Fluorescent particle tracing	45.15 μL/min at 9 kPa (60 times press/min)	This study
			Estimating method based on driven volume	About 138 μL/min at 30 kPa	

References of Supporting information:

1. C. H. Lu, T.-S. Shih, P.-C. Shih, G. P. Pendharkar, C.-E. Liu, C.-K. Chen, L. Hsu, H.-Y. Chang, C.-L. Yang and C.-H. Liu, Lab on a Chip, 2020, 20, 424-433.
2. S.-M. Ha, W. Cho and Y. Ahn, Microelectron Eng, 2009, 86, 1337-1339.
3. J. Ni, F. Huang, B. Wang, B. Li and Q. Lin, J Micromech Microeng, 2010, 20, 095033.

Tab. S2 Process scheme comparison for mass manufacturing of valved micropumps

Processing Method of Valved Micropumps	Process scheme	Main concerns in mass manufacturing					Main conclusion
		Alignment problem	Multi-layer PDMS bonding strength	Movement of the one-way valve bodies	Consistency of pump structures	Repeatability of molds	
Conventional methods	Photolithography molds; Multi-layer PDMS assembled by plasma treatment	Short alignment time; high difficulty	Uneven bonding **(Fig. 3c)**	Unable to ensure (easy lead to the valve body bond with other PDMS)	Unable to ensure (Too much manual processing and difficult alignment)	Low (Brittleness of UV cured structures)	Not suitable for mass manufacturing of valved micropumps
This study	Photolithography molds; multi-step PDMS curing; Controllable separation strategy (vacuum coating method)	Sufficient alignment time; **Easy** (Actually, it's mold alignment)	Uniform and good bonding strength **(Fig. 3c)**	Completely enable valve body movement **(Fig. 2c)**	**74% yield rate**; (Main cause: defects in Mold1 & Mold2 **(Fig. S10)**)	**Low** (Brittleness of UV cured structures in Mold1 and Mold2)	**Fully feasible when using metal molds for mass manufacturing**

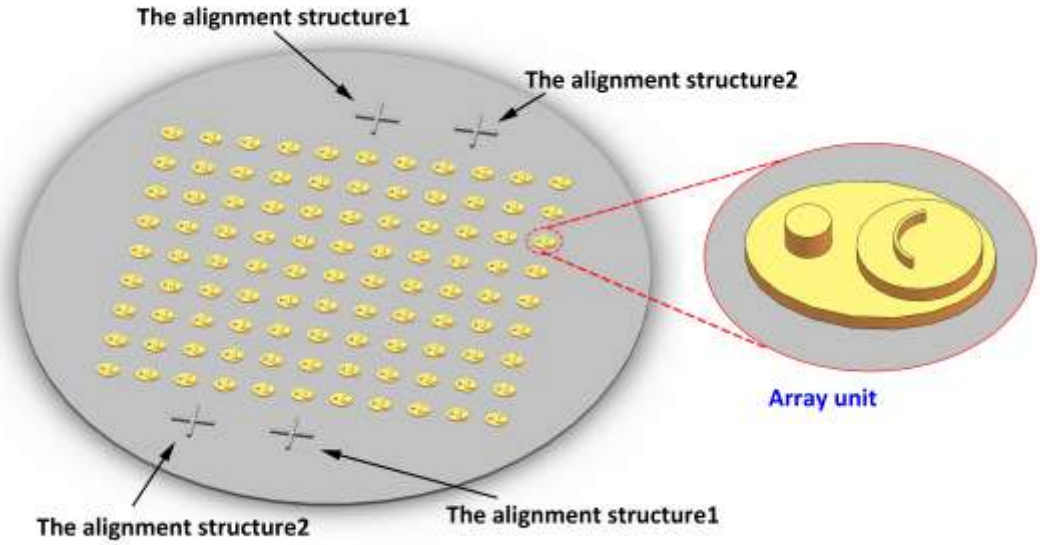

Fig. S1. Schematic of the Mold1. The array units on the Mold1 were used to form the internal cavity of the micro-pump units, the alignment structure1 was used to align with the metal mask in step4, and the alignment structure2 was used to align with the Mold2 in step6.

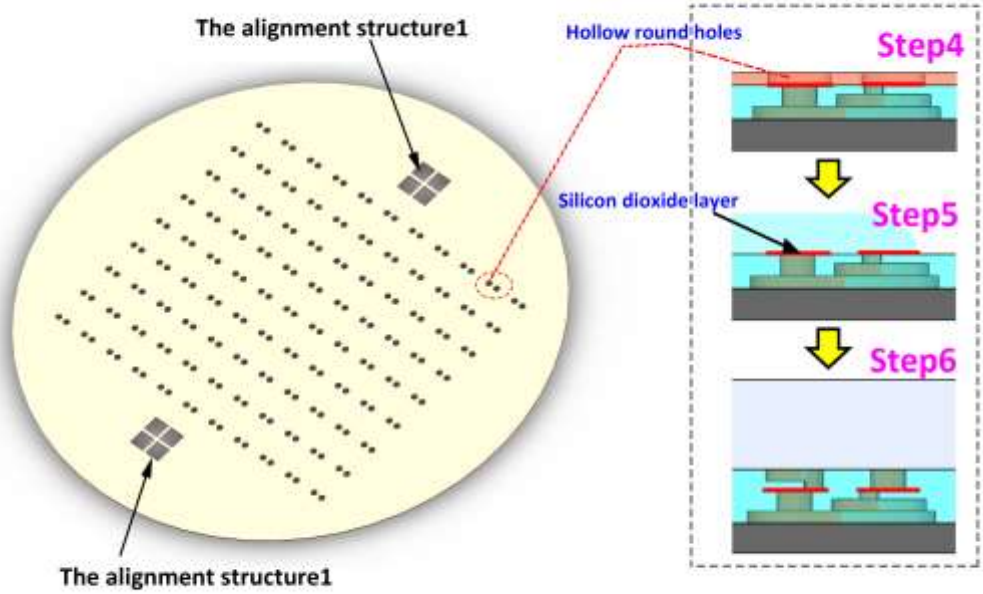

Fig. S2. Schematic of the metal mask. The alignment structure1 was used to align with the Mold1 in step4 (Fig. 1a). The Silicon dioxide layer in red lines was formed through the vacuum coating machine.

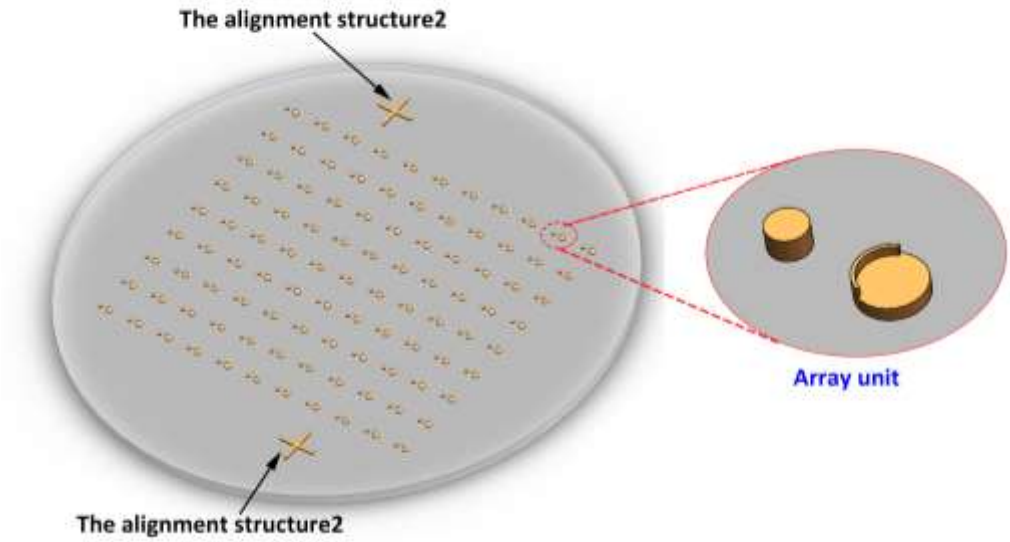

Fig. S3. Schematic of the Mold2. The array units on the Mold2 were used to form the inlets and outlets of the micro-pump units, and the alignment structure2 was used to align with the Mold1 in step6.

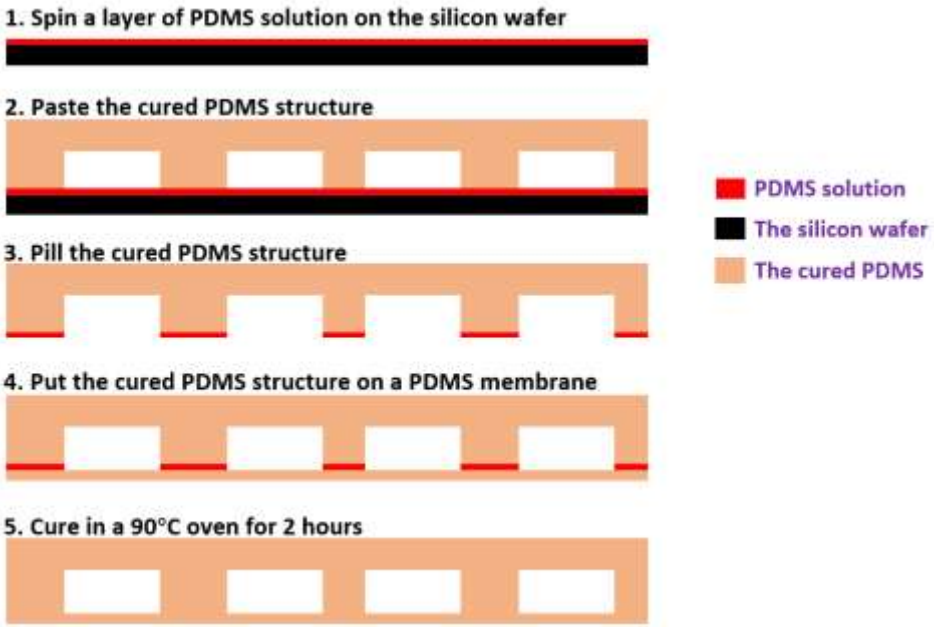

Fig. S4. Integrated curing technology of multi-layer PDMS structure. The PDMS solution layer was formed at 6000 r/min for 3 min, and its thickness was less than 3 μm.

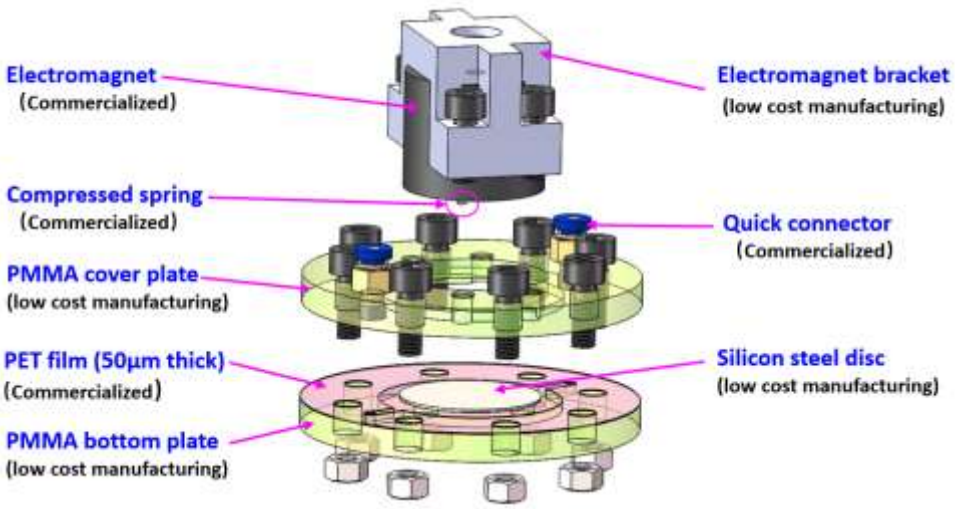

Fig. S5. 3D design diagram of the fluid pressure generating device (corresponds to Fig. 4b).

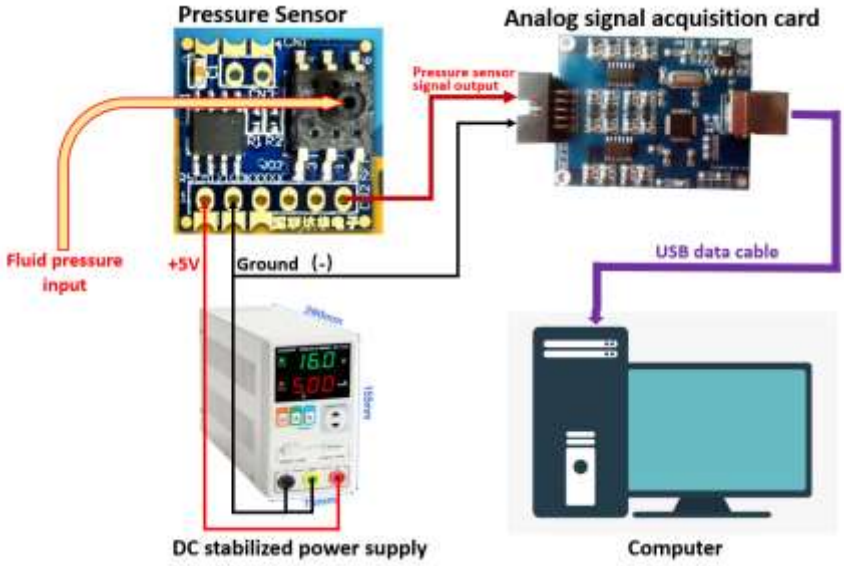

Fig. S6. Schematic diagram of the microfluidic pressure measurement platform.

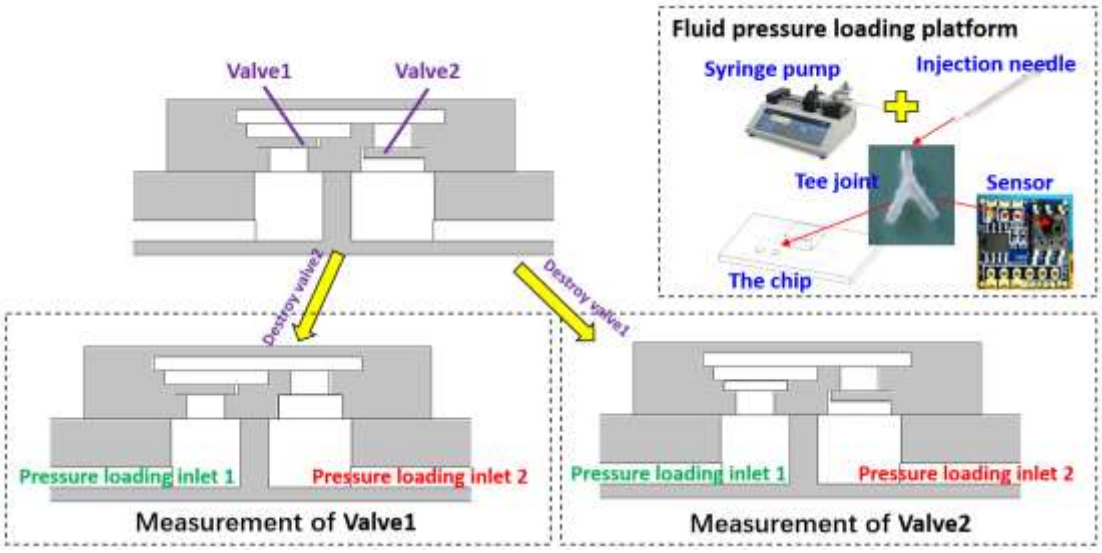

Fig. S7. The measurement of one-way valves' opening pressure and reverse cut-off pressure. The valve opening pressure was obtained by loading the pressure from the fluid pressure loading platform into the pressure loading inlet 1. The reverse cut-off pressure was obtained by loading the pressure from the fluid pressure loading platform into the pressure loading inlet 2.

Fig. S8. The fluid velocity measurement method on the chip based on the fluorescent microparticle. The motion video of the polystyrene particles was acquired under a fluorescence microscope, and the video editing software was used to obtain the picture of each frame. And then the Image-pro-plus software was used to measure the moving distance of each fluorescent particle at each time interval to obtain the particle motion speed. Multiple fluorescent particles in the microchannel were selected to calculate the average velocity of the fluid. Scale bar: 500 μm.

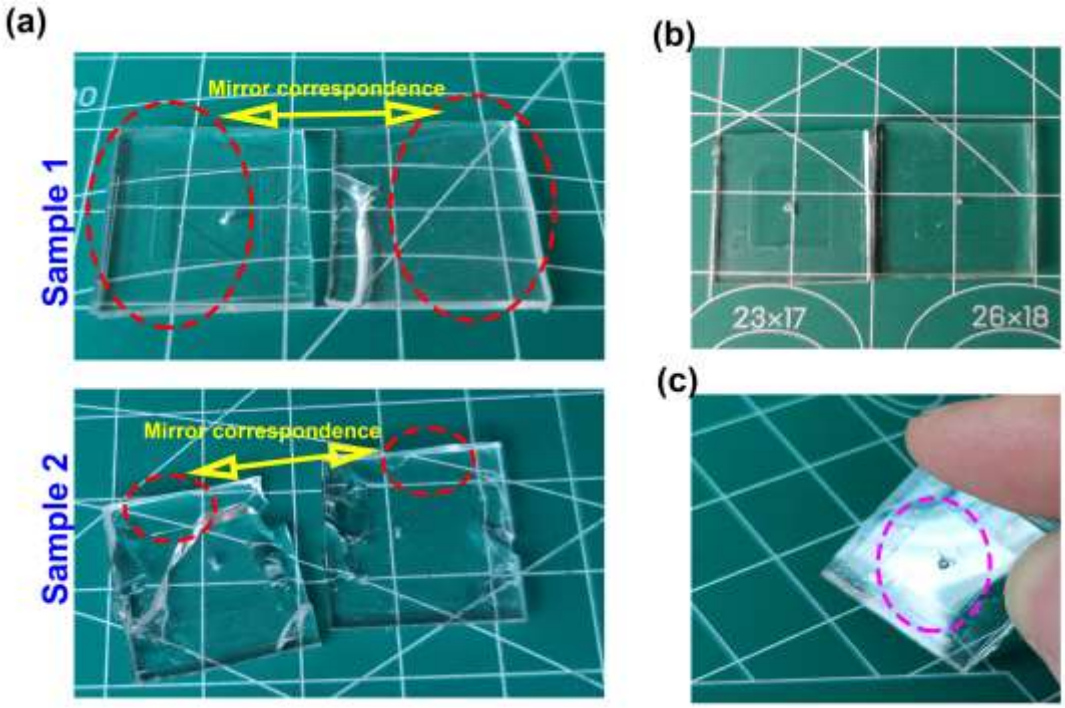

Fig. S9. (a) Tearing surface pictures of the PDMS structure (Fig. 3b) assembled through the plasma treatment, and the PDMS layers at the red dashed line did not obtain effective bonding. **(b)** Tearing surface picture of the PDMS structure (Fig. 3b) assembled through the integrated curing process (Fig. S4). **(c)** The PDMS structure assembled through the integrated curing process was damaged at the pressure port during the pressure-bearing test, resulting in the inability to obtain higher maximum pressure data.

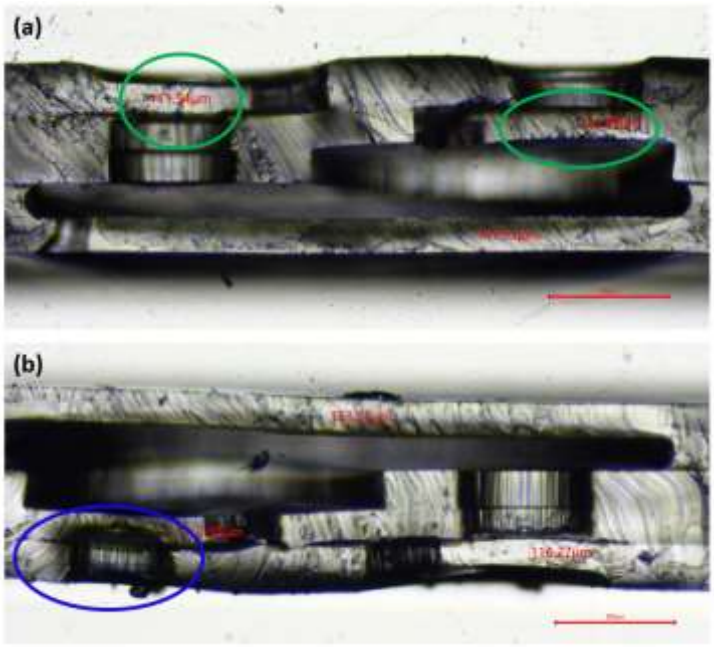

Fig. S10. The pictures of the defective micropump units. The green ellipses indicate the size defect of the micropump unit, and the blue ellipse indicates the structural defect of the micropump unit. Scale bar: 500 μm.

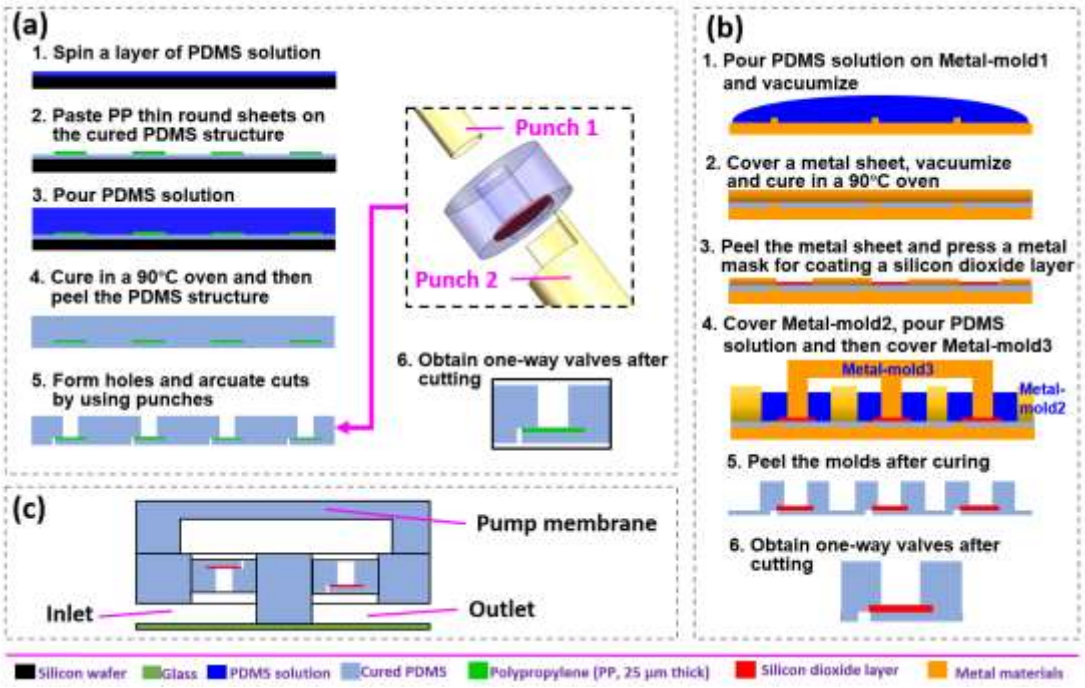

Fig. S11. (a) Schematic diagram of a processing method of one-way valves based on punches. **(b)** Schematic diagram of a processing method of one-way valves based on metal molds. **(c)** The one-way valves can be used to assemble a pump.

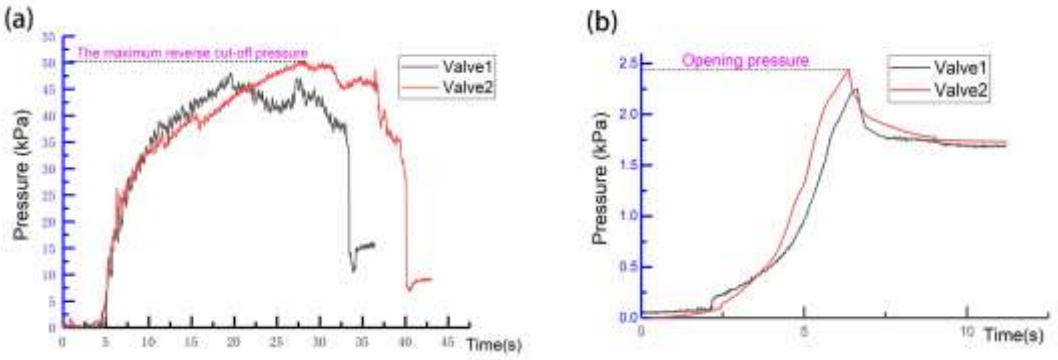

Fig. S12. (a) Pressure change curve for evaluating the maximum reverse cut-off pressure of the Valve1 and the Valve2. **(b)** Pressure change curve for evaluating opening pressure of the Valve1 and the Valve2. The above curves were obtained through the experimental platform shown in Fig. S7.

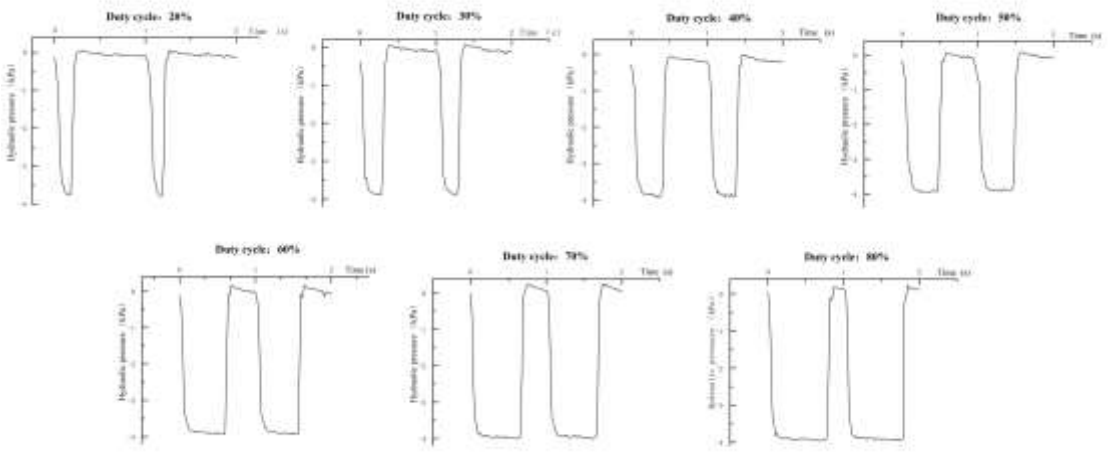

Fig. S13. The fluid pressure waveform output by the fluid pressure generating device at different duty cycles; the frequency of the input square wave electrical signal is 1 Hz.

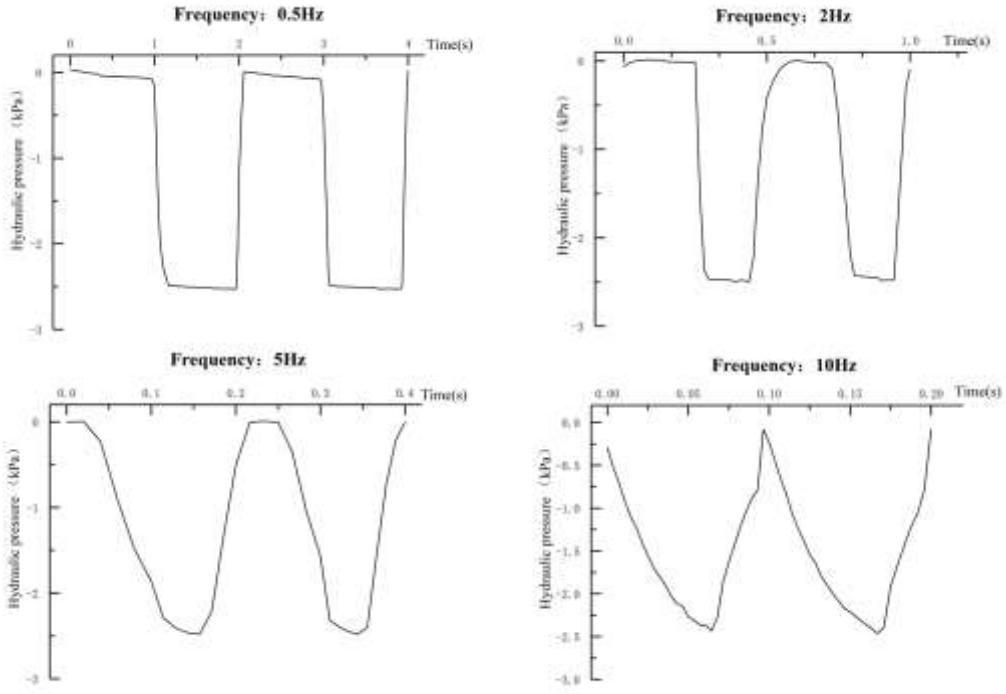

Fig. S14. The fluid pressure waveform output by the fluid pressure generating device at different frequencies; the duty cycle of the input square wave electrical signal is 50%.

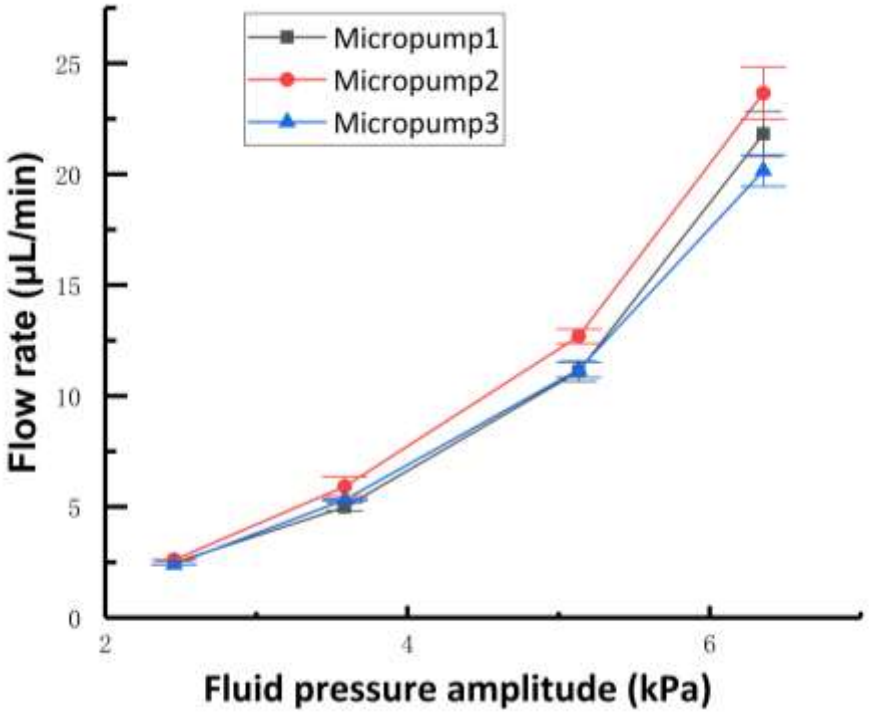

Fig. S15. The change curve of the flow rate of three different micropumps with different pressure amplitudes. The fluid pressure generated by the relative device (Fig. 4b) was loaded into the pump and the frequency was 1Hz and the duty cycle was 50%.

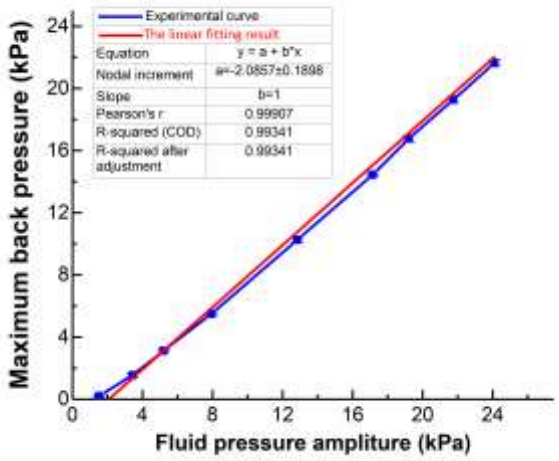

Fig. S16. Linear fitting result of the change curve of the maximum back pressure with the fluid pressure amplitude.

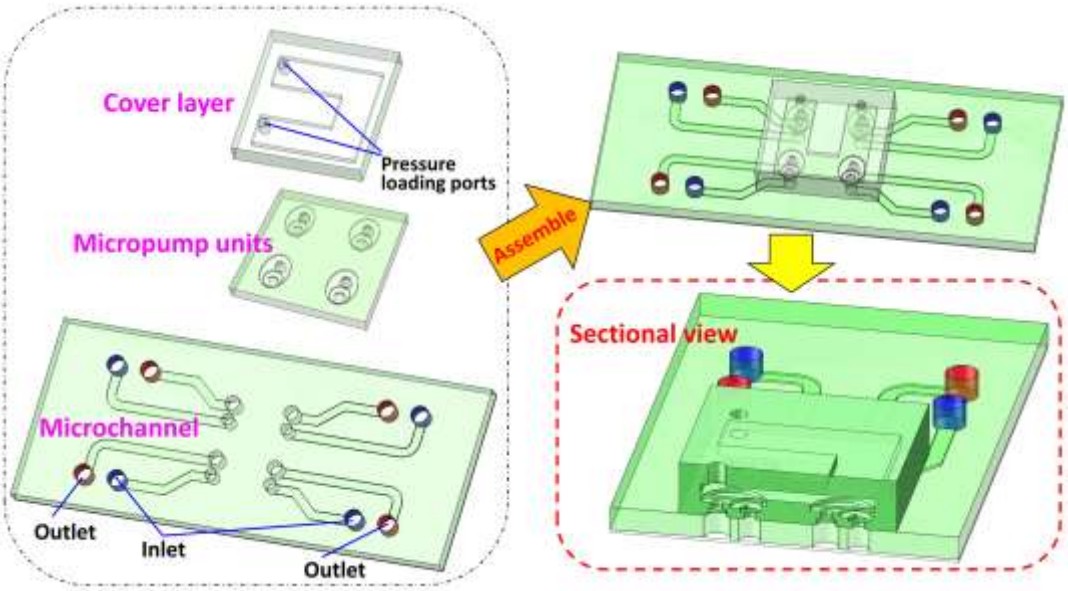

Fig. S17. Four micropump units were integrated into the chip to meet the needs of high-throughput fluid driving. The fluid pressure output by the fluid pressure generating device was loaded into the chamber of the cover layer through the pressure loading ports to drive the micropumps.